Numerical Approach for Convective Magnetohydrodynamic (Mhd) Nanofluid Flow with Impermeable Stretching Surface

Abubakar Assidiq Hussaini*, Abdullahi Madaki Gamsha†, Sanusi Kabiru Alaramma‡, Aminu Barde§, Isah Abdullahi**

Abstract

This research explores the convective magnetohydrodynamic (MHD) boundary layer flow of nanofluid, past a nonlinear impermeable stretchable surface of variable thickness. The flow is influenced by linearly stretching the surface with internal heat generation or absorption and by the presence of Soret diffusivity and impermeability of the surface. The mathematical expressions are accomplished via boundary layer access. The Partial differential systems (dimensional systems) are transformed into Ordinary differential systems (non-dimensional systems). The governing non-linear profiles of momentum, temperature, and nanoparticles concentration have been solved numerically by using the Runge–Kutta–Fehlberg method along with the shooting technique. Numerous emerging Physical parameters which are involved in the system are interpreted by the table of values. however, the effects of Soret diffusivity, as well as impermeability of the surface, were numerically studied and analyzed. According to the result we found, it is revealed that higher impermeability of the surface results in the reduction of velocity distribution, as well as Nusselt number. Whereas, Effects of Soret diffusivity on the profiles of nanoparticles as well as the temperature were found to have reverse effects. It was observed as well that higher values of impermeability parameters enhanced the temperature of the system as well as the system's concentration. Hence, temperature, momentum, Nusselt number as well as Sherwood number are found to be decreasing functions.

***Keywords*:** Impermeability, heat generation/absorption, Convective, Nanofluid, Stretching surface

Introduction

A nanofluid is a fluid containing nanometer- sized particles which are usually called nanoparticles. These fluids are engineered colloidal suspensions of nanoparticles in a base fluid. The nanoparticles that are

* Department of Mathematical Sciences, Abubakar Tafawa Balewa University, PMB 0248, Bauchi. Nigeria. alhajhabu@gmail.com
† Department of Mathematical Sciences, Abubakar Tafawa Balewa University, PMB 0248, Bauchi, Nigeria. abdulmdk119@gmail.com
‡ Department of Mathematical Sciences, Abubakar Tafawa Balewa University, PMB 0248, Bauchi, Nigeria. sanusikabiratbu@yahoo.com
§ Department of Mathematical Sciences, Abubakar Tafawa Balewa University, PMB 0248, Bauchi, Nigeria. bardealamin@yahoo.com
** Department of Mathematical Sciences, Abubakar Tafawa Balewa University, PMB 0248, Bauchi, Nigeria. Isahabdullahi7474@gmail.com

mostly used in nanofluids are typically made of metals, oxides, carbides, or carbon nanotubes.

They have the capability of increasing the thermophysical properties of the base fluids. Common base fluids include water, ethylene glycol and oil. Three properties that make nanofluids promising coolants are as follows the increase thermal conductivity, the increased heat transfer and the increased critical heat flux. Previous studies shown that relatively small quantity of nanoparticles can enhance thermal conductivity of base fluids to a large extent. These are some nanomaterials and their base fluids Alumina nanoparticles and copper oxide nanoparticles (water), Titanium nanoparticles and silver nanoparticles (water), Multiwall carbon nanotubes and magnesium oxide nanoparticles (Engine oil), Multiwall carbon nanotubes and zinc oxide nanoparticles (Engine oil). Magnetic nanofluids (Ferro fluids), are the fluids which consists of colloidal mixture of superparamagnetic nanoparticles suspended in a nonmagnetic carrier fluid, which constitute a special class of nanofluids that exhibit both magnetic and fluid properties.

Magnetic nanoparticles (MNPs) have shown promise in a number of biomedical applications, including: magnetic hyperthermia, enhancing magnetic resonance imaging (MRI) data, supplementing tissue engineering efforts and improving the delivery of drugs which are too difficult to reach micro inches. Diagnosis and treatment of cancer and infectious diseases alongside enhancing tissue engineering techniques, etc. The term nanofluid was first employed by Choi (1995), in his effort to propose a new way to make an improvement in the heat transfer. He achieved it by scattering particles of Nano size in a base fluid. The convective transfer phenomena in nanofluids were studied by Buongirno (2006). Khan et al (2010) studied the two-dimensional stretchable flow of nanofluids. After which, this analysis was extended, where convective boundary condition was considered by Makinde et al (2011).

Many Scientists and engineers are interested in the investigation of nanofluid flow in various aspects. Some of the recent studies includes the following: Sheikholeslami et al (2014), Zeeshan et al (2014), Hayat et al (2015), Abbasi et al (2016), to mention but few. Another research includes Jawad et al (2019) who studied the Sisko nanofluid film over an unsteady stretchable surface in a uniform magnetic field. They determined the effects of Brownian motion and thermophoresis, after they applied the Homotopy analysis on the system of heat and mass transfer. The influence of magnetic field on the boundary layer flow of Newtonian Sisko nanofluid flow over a wedge was studied by Macha et al. (2017), Pal et al. (2019), they added first- order chemical reaction on the boundary layer flow together with non-linear thermal radiation of nanofluid past a plate

which is saturated in a porous medium to the effects of magnetic field. The melting effect, heat generation or absorption, thermal radiation of Sisko nanofluid over a stretchable surface was established by Mabood et al (2019).

The influence of the physical properties of the magnetic nanofluid flow and heat transfer has been studied by several researchers such as Daniel et al (2018), Malik and Khan (2018), Khan et al (2018). Ali et al. (2020) studied the effects of Lorentz's forces, non-uniform sink source, chemical reaction, thermal radiation and thermophoresis on Sisko nanofluid over a curved surface. Analysis on MHD nanofluid towards non-linear stretching surface with variable thickness in the presence of an electric field was conducted by Ishak et al. (2011). Al-sanea et al. (2014) conducted an extensive experiment in order to confirm the influence of variable thermal conductivity and magnetic field in an unsteady Sisko nanofluid flow over a stretching sheet together with heat generation/absorption respectively. Other relevant studies include the work by Ghadikolaei et al. (2018) on the convective MHD flow of Casson nanofluid over a non- linear permeable stretching surface. Just of recent, there are numerous researches which paid much attention about the natural phenomenon of convective MHD as well as nanofluids, some of which are: Madaki et al. (2016), (2017), (2018), (2019), (2020), (2021). The effects of Heat generation/absorption on MHD nanofluid flow was conducted by Hussaini et al. (2021). Kothandapani and Prakash (2014), (2015) investigated the intrauterine fluid motion in a non- pregnant uterus which was caused by myometrial contractions in a peristaltic- type fluid motion as well as myometrial contractions which might be occurred in both directions. It was later discovered that the intrauterine fluid flow in a sagittal cross section of the uterus which was disclosed in a narrow channel enclosed by two (2) fairly parallel walls along with wave trains different amplitudes and phase.

In spite of the substantial importance of Soret diffusivity as well as impermeability of a stretching surface in the fields of science and engineering, for their numerous applications, yet to the best of the authors' knowledge there was no attempt so far to discuss their effects on this particular model. To this end, the main aim of this research is to investigate and vividly discuss on the influence of both Soret diffusivity and impermeability of stretching surface over internal heat generation/absorption on nanofluid.

Mathematical analysis

The research Considered boundary-layer flow of a nanofluid in two-dimension, which is passed through a heated stretching surface, on which convective boundary conditions are applied. The velocity at the wall (i.e., the sheet's surface) is considered toward the origin moving in the x- direction, which implies Uw = ax, such that a is greater than zero, x is considered as the coordinate placed at the edge of the sheet. The physical model below (fig.1) explains this concept physically.

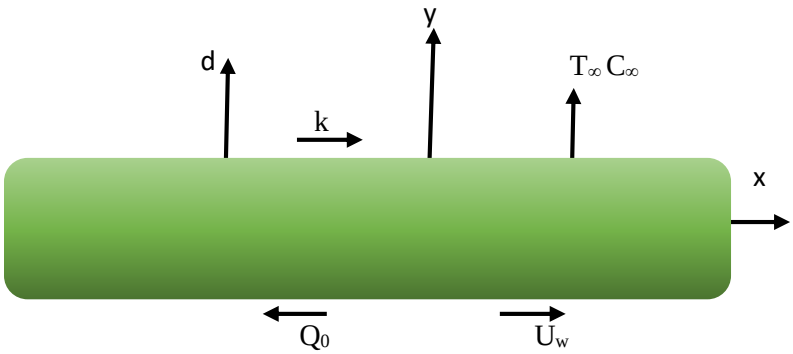

Figure 1: Physical model and coordinate system

The free stream velocity of the fluid is considered to be equals to (bx). The impermeability is exposed to flow naturally in the y direction so as to go along with the fluid's flow direction. It was assumed that the magnetic field which was as the result of polarization of different charges is neglected and the external electrical field is taken to be zero. Then the numerical analysis is done based on Soret diffusivity and Impermeability together with other physical parameters in the model. The temperature at the wall is denoted by T_w while the quiescent temperature of the fluid is denoted by T_f.

Below is the mathematical model that describes the Momentum profile, the temperature profile, as well as nanoparticle concentration profile as described by Hussaini et al. (2021) which explains flow of the fluid:

$$\frac{\partial \Psi}{\partial y}\frac{\partial^2 \Psi}{\partial x \partial y} - \frac{\partial \Psi}{\partial x}\frac{\partial^2 \Psi}{\partial y^2} = U_\infty \frac{\partial U_\infty}{\partial x} + v_f \frac{\partial^3 \Psi}{\partial y^3} + \frac{\sigma_e B_0^2}{\rho_f}(u - U_\infty) + \frac{\mu_e}{k}u, \quad (1)$$

$$\frac{\partial\Psi}{\partial y}\frac{\partial T}{\partial x}-\frac{\partial\Psi}{\partial x}\frac{\partial T}{\partial y}=\alpha\frac{\partial^2 T}{\partial y^2}+\frac{v_f}{C_f}\left(\frac{\partial^2\Psi}{\partial y^2}\right)^2+\frac{\sigma_e B_0^2}{(\rho C)_f}(U_\infty-u)^2+\tau\left\{D_B\frac{\partial T}{\partial y}\frac{\partial C}{\partial y}+\frac{D_T}{T_\infty}\left(\frac{\partial T}{\partial y}\right)^2\right\}++\frac{16\sigma^* T^3}{3(\rho C)_f k^*}\frac{\partial^2 T}{\partial y^2}+\frac{Q}{\rho_{nf}}(T-T_\infty), \quad (2)$$

$$\frac{\partial\Psi}{\partial y}\frac{\partial C}{\partial x}-\frac{\partial\Psi}{\partial x}\frac{\partial C}{\partial y}=(D_{TC}+D_B)\frac{\partial^2 C}{\partial y^2}+\frac{D_T}{T_\infty}\frac{\partial^2 T}{\partial y^2}+[-K_1(C-C_\infty)], \quad (3)$$

These are the boundary conditions for the fluid's flow:

$$u=ax, v=0, C=C_{w.}, -k\frac{\partial T}{\partial y}=h(T_f-T)aty=0$$

$$u=bx, v=0, C=C_\infty, T=T_\infty asy\to\infty. \quad (4)$$

$\Psi(x,y)$: is the stream function such that $u=\frac{\partial\Psi}{\partial y}$ where $v=-\frac{\partial\Psi}{\partial x}$, u,v described velocities along the two directions via x and y. σ_e: considered as the fluid's electrical conductivity, ρ: density, α: fluid's thermal diffusivity and B_0: magnetic field, T: the fluid's temperature, ρ_f is the density of the nanofluid, $(\rho C)_f$: as the fluid's heat capacity, Cf the skin friction coefficient, D_T is the thermophoresis diffusivity, k_1, D_B, $\tau=(\rho C)_p/(\rho C)_f$ are the impermeability, the Brownian diffusion and the ratio of the heat capacity to the fluid's effective heat capacity of the nanoparticle. We applied the Roseland approximation (1931) in order to assess the value for radiative heat parameter as it appeared in the temperature profile above $q_r=-\frac{4\sigma^*\partial T^4}{3k^*\partial y}$. These are the non- dimensional quantities as used by Khan and Pop., (2010).

$$u=axf'(\eta), \Psi=xf(\eta)\sqrt{av_f}, \phi(\eta)=\frac{C-C_\infty}{C_w-C_\infty}, T=\theta T_w, \eta=y\sqrt{\frac{a}{v_f}},,$$

$$\theta(\eta)=\frac{T-T_\infty}{T_f-T_\infty}, C=\phi C_w, v=f(\eta)\sqrt{av_f}, \quad (5)$$

The eqs. (1) – (4) are taken one after the other together with the dimensionless quantities in eq. (5), which after the substitutions and expansion will yield the desired ordinary differential equations as given below:

$$f'''+ff''-f'^2+A^2+M(A-f')+k_1f'=0, \quad (6)$$

$$\{[1+N\{1+(\theta_c-1)\theta\}^3]\theta'\}'+Pr[f\theta'+Nb\theta'\phi'+Nt\theta'^2+Ecf''^2+MEc(A-f')^2+\lambda\theta]=0, \quad (7)$$

$$\phi''+\frac{Le}{d}f\phi'+\frac{Nt}{dNb}\theta''-\gamma\phi=0, \quad (8)$$

$$Le = \frac{v_f}{D_B}, Nb = \frac{\tau D_B(C_w - C_\infty)}{v_f}, Nt = \frac{\tau D_B(T_f - T_\infty)}{v_f T_\infty},$$
$$Bi = \frac{h(V_f/a)^{1/2}}{k}, Ec = \frac{U_w^2(x)}{C_n(T_w - T_\infty)}, \frac{k_1 v_f(C_w - C_\infty)}{aD_B C_\infty}$$

Here, the prime constitutes the derivatives of the functions (one prime means 1st derivative, double primes means 2nd derivatives and triple primes means 3rd derivatives) of which all of them are with respect to $\eta, M = \frac{\sigma_e B_0^2}{a\rho_f}$ stand for the magnetic parameter, $k_1 = \frac{ax\mu_e}{k}$ is the Permeability parameter, $A = \frac{b}{a}$, $Pr = \frac{v_f}{\alpha}$, $\lambda = \frac{Q}{aT_w\rho_{nf}}$, $N = \frac{16\sigma^* T^4}{3kk^*}$, stands as the ratio of the rates of free stream velocity and the velocity of the sheet, the Prandtl number, heat generation/absorption parameter and radiation parameter respectively, and $d = \left(\frac{N_d}{D_B} + 1\right), where N_d = D_{TC}$.

The non- dimensional temperature in Eq. (5) above can be expressed as follows:$T = T_\infty(1 + (\theta_c - 1)\theta)$ in this expression $\theta_c = \frac{T_f}{T_\infty}$. which can also be expressed as follows based on the terms we have in eq. (2) above

$$\alpha\left(\frac{\partial}{\partial y}\right)\left[\frac{\partial T}{\partial y}(1 + N(1 + (\theta_c - 1)\theta)^3)\right] + \frac{a(T_f - T_\infty)}{Pr[(1 + N(1 + (\theta_c - 1)\theta)^3)\theta']'}$$

Now applying the following boundary conditions on Eqs. (6)– (8)
$f(0) = 0, f'(\infty) = A, f'(0) = 1, \theta'(0) = -Bi[1 - \theta(0)], \theta(\infty) = 0, \phi(0) = 1, \phi(\infty) = 0,$ (9)

Below are the definitions of the involving parameters in the model from eqs. (6) to eqs. (10): Nb, Ec, γ, Le, Nt are the Brownian motion parameter, the Eckert number, and chemical reaction parameter, Lewis number, thermophoresis parameter, respectively. Other very important accents are as follows: The Nusselt number, the Sherwood number, wall heat flux (q_w) as well as wall mass flux (q_m) respectively, which are expressed as follows:

$$Nu_x = \frac{xq_w}{k(T_w - T_\infty)} \Rightarrow -\sqrt{Re_x}[1 + N\theta_c^3]\theta'(0) = Nur,$$
$$Sh = \frac{xq_m}{D_B(C_w - C_\infty)} \Rightarrow -\sqrt{Re_x}\phi'(0) = Shr. q_w = -k\left(\frac{\partial T}{\partial y}\right)_{y=0} + (q_r)_w = -k(T_w - T_\infty)(a/v_f)^{1/2}[1 + N\theta_c^3]\theta'(0),$$
(10)

$$q_m = -D_B \left(\frac{\partial C}{\partial y}\right)_{y=0} = -D_B(C_w - C_\infty)(a/v_f)^{1/2}\phi'(0),$$

Results and discussion

Non-linear ordinary differential equations Eqs. (6), Eqs. (7), and Eqs. (8). Where evaluated by the use of Runge–Kutta- Fehlberg method (the fourth order) together with shooting technique using Maple along with these boundary conditions which are given in Equation (9), for various values of the physical emerging parameters such as: Magnetic parameter (M), Lewis number $(Le,)$ $(Pr), (R), (k), (Nb), (Nt)$, Prandtl number, radiation parameter, chemical reaction, Brownian motion, thermophoresis parameter, respectively. The profiles of velocity, temperature as well as concentration are solved numerically for variable values of emerging physical parameters which are involved in the model. The result is represented graphically and on table of values and for different values of the Nusselt number profile, Sherwood number profile, velocity profile, temperature profile and concentration profile. Our results are confirmed to be valid as displayed in table1, for different values of the physical parameters which are in the model while considering both permeability and Soret diffusivity parameters (d and $k_1 = 0$) = 0. Hence, there is a great engrossing concurrence allying this result and the preceding researches.

Table1

Validation of the obtained results by considering some values of the reduced Nusselt number $-\theta'(0)$, as well as the values of the reduced Sherwood number $-\phi'(0)$, where the parameters with the given fixed values are: $Nb = Nt = 0.5$ and $\gamma = R = 0$

Pr	***Bi***	***Le***	**Mushtaq et al. (2014)**		**Madaki et al. (2019)**		**Hussaini et al. (2020)**		**Present study**	
			$-\theta'(0)$	$-\phi'(0)$	$-\theta'(0)$	$-\phi'(0)$	$-\theta'(0)$	$-\phi'(0)$	$-\theta'(0)$	$-\phi'(0)$
2	0.1	5	0.08062	1.55543	0.08068	1.55554	0.08061	1.55543	0.08061	1.5554
5	0.1	5	0.07344	1.59833	0.07339	1.59790	0.07345	1.59831	0.07345	1.5983
10	0.1	5	0.03867	1.72932	0.03857	1.72927	0.03868	1.72928	0.03868	1.72928
5	5	5	0.14756	1.69139	0.14754	1.69136	0.14756	1.69136	0.14756	1.69136
5	10	5	0.15498	1.71222	0.15475	1.71223	0.15498	1.71222	0.15498	1.71222
5	5	5	0.15556	1.71437	0.15543	1.71441	0.15565	1.71438	0.15565	1.71438
5	∞	5	0.15572	1.71461	. . .	. . .	0.1557	1.71462	0.1557	1.71462
5	0.1	10	0.06468	2.39201	0.06466	2.39211	0.06468	2.39196	0.06468	2.39196
5	0.1	15	0.05998	2.99003	0.05710	2.98988	0.05999	2.98993	0.05999	2.98993

From Table 2 above it is clear that, the influence of both Heat generation/absorption parameter and Biot number are depicted on the reduced Nusselt number profile $-\theta'(0)$ along λ *and Bi* considered differently (uniquely). It can be observed that the reduced Nusselt number decreases remarkably.

The reduced Sherwood number $-\phi'(0)$, notably remained constant for each value. Moreover, increase in the values of magnetic

parameter (M) and the Eckert number (Ec) neither influence the temperature gradient nor the concentration, this is clearly depicted on table 3.

Table 2

Effects of Heat generation/absorption parameter (λ) and Biot number (Bi) on reduced Nusselt number, (Nur) $-\theta'(0)$ *and reduced Sherwood number, (Shr)* $-\phi'(0)$*, when R=1, M=0,* θ_w*=0.02, Nb=1,* Pr =1, k= 0.6089

$\lambda =$	**0**	**0.1**	**0.5**	**0.8**	**1**
$Bi =$	0.01	0.01	0.02	0.02	0.10
$-\theta'(0) =$	0.00971	0.00972	0.0191	0.0192	0.0851
$-\phi'(0) =$	0.78032	0.78032	0.78032	0.78032	0.78032

Table 3

Effects of Magnetic parameter [M] and Eckert number [Ec], on the Sherwood number, (Shr) $-\phi'(0)$ *and Nusselt number, (Nur)* $-\theta'(0)$ *and when R=1,* λ*=1,* θ_w*=0.02, Nb=1,* Pr =1, k= 0.6089

$M =$	**0**	**5**	**6**	**8**	**10**
Ec =	0.0	0.0	0.1	0.1	0.3
$-\theta'(0) =$	0.08512	0.08512	0.08512	0.08512	0.08512
$-\phi'(0) =$	0.7803	0.7803	0.7803	0.7803	0.7803

Table 4

Effects of Prandtl number (Pr) and Magnetic Parameter (M) to the Temperature $-\theta'(0)$ *profile as well as the Nanoparticle concentration* $-\phi'(0)$ *profiles, considered for,* Pr =1, *R=1,* λ*=1, Nb=1,* k= 0.6089, θ_w*=0.02*

$Pr =$	**0**	**5**	**10**	**20**	**25**	**27**
M =	0.0	0.0	5.0	5.0	6.0	6.0
$-\theta'(0) =$	0.0852	0.0827	0.0716	0.0346	0.0177	0.0130
$-\phi'(0) =$	0.7803	0.7803	0.7803	0.7803	0.7803	0.7803

From Table 4 above, it can be observed that, increase in the values for Prandtl number (Pr) as well as magnetic parameter (M), decrease the temperature significantly but the concentration profile remained constant. furthermore, it can be seen that whenever there is an increase in the values of Prandtl number together with Magnetic parameter this will result in lowering the temperature gradient, which directly amplifies the heat transfer significantly.

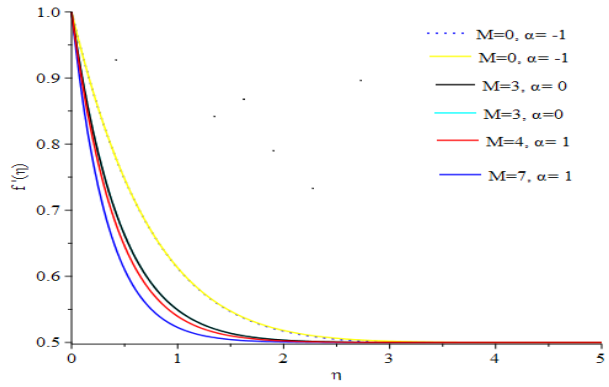

Figure 2: Influence of (M) on velocity

Figure 2. shows the influence of (M) alongside with impermeability (α) on the profile of Velocity: fluid's Velocity is physically reducing with the increase of Magnetic parameter irrespective of the value of impermeability parameter (increase or decrease). On the other hand, *Figure3.* shows the effects of Magnetic parameter (M) and impermeability parameter (α) to the profile of Nusselt Number. the Nusselt number of the fluid physically decreased whenever there is an increase in Magnetic parameter. From figure4. It can be seen that there is a decrease in the fluid's Sherwood number, with the increment in magnetic parameter not minding the value of the impermeability parameter. It can be seen from Figure5. (effects of Soret diffusivity parameter as well as the wall temperature parameter) that the fluid's Temperature is decreasing with increase in Soret diffusivity parameter when the wall Temperature is decreased. Whereas, the fluid's temperature increases with increment of Soret diffusivity parameter when the wall temperature is increased.

Figure 6 displayed the effects of Soret diffusivity and Wall Temperature on the concentration profile, where it can be observed that the fluid's concentration increases with the increment in the value of Soret diffusivity irrespective of either increase or decrease in the value of the wall temperature. Furthermore, on figure 7. (effects of Soret diffusivity to the Nusselt number profile). whereby, increment in the values of Soret diffusivity significantly decreases the Nusselt number.

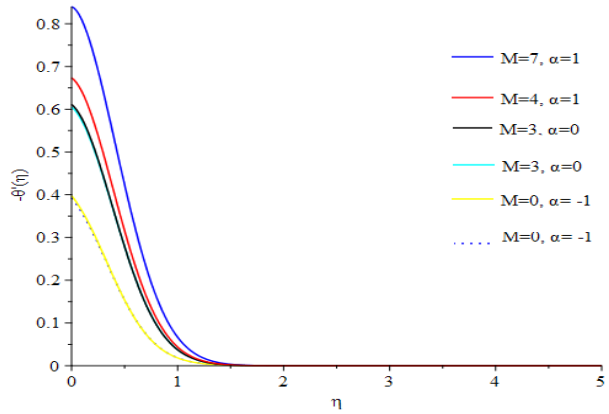

Figure 3: Influence of (M) on the Nusselt number.

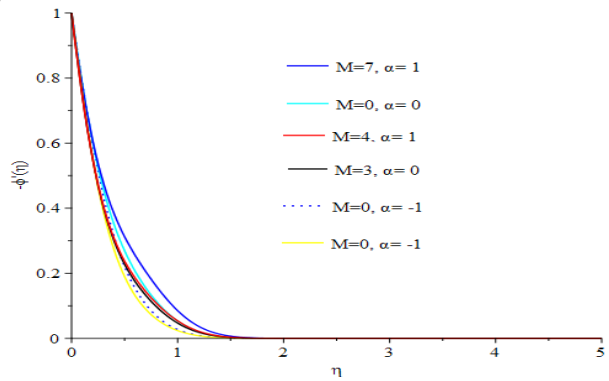

Figure 4: Influence of the Magnetic Parameter (M) to the Sherwood number

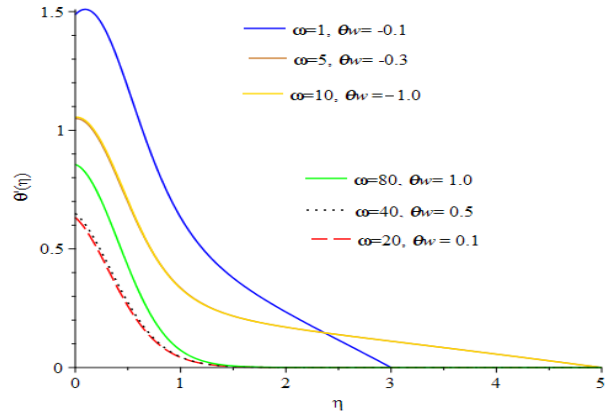

Figure 5: Influence of Soret diffusivity parameter (ω) to the Temperature

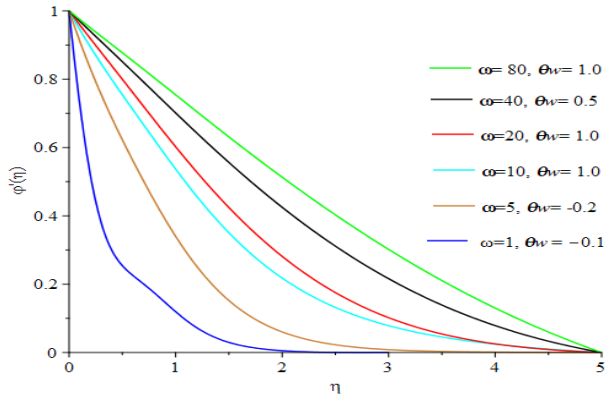

Figure 6: Effects of Soret diffusivity parameter (ω) to the Concentration

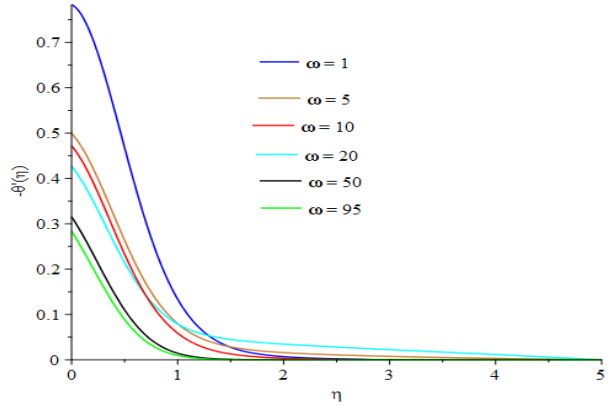

Figure 7: Effects of Soret diffusivity parameter (ω) to the Nusselt Number

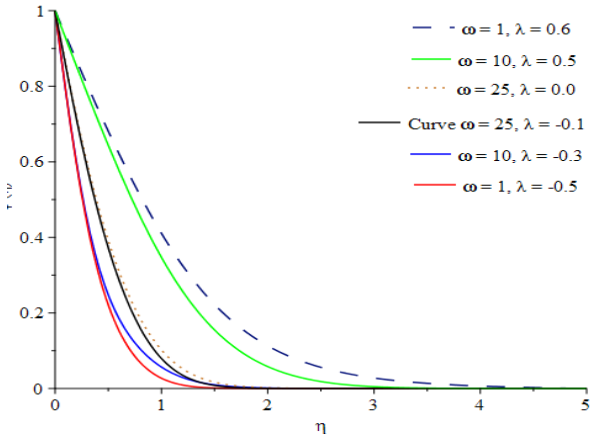

Figure 8: Effects of Soret diffusivity parameter (ω) and Heat generation/absorption parameter (λ) to the Sherwood number

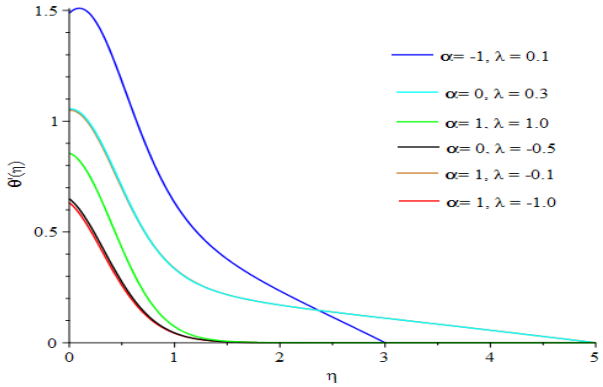

Figure 9: Effects of Impermeability parameter (α) and Heat generation/absorption parameter (λ) to Temperature

As regards figure 8, (effects of Soret diffusivity with Heat generation/absorption parameter on Sherwood number profile): increasing the value of Soret diffusivity parameter decreases the Sherwood number when heat generation ($\lambda > 0$) is applied to the system, whereas, increase in the values of Soret diffusivity parameter increases the Sherwood number, on the other hand, when heat absorption ($\lambda < 0$) is applied to the system. From figure9. (effects of impermeability parameter with heat generation/absorption on temperature profile) increment in the values of impermeability parameter brings about a decrement on the profile of temperature $\theta'(0)$, irrespective of whether it's ($\lambda > 0$) or heat absorption ($\lambda < 0$).

Conclusion

A numerical study of the boundary layer flow in a nanofluid induces as a result of the motion of a linearly stretching sheet has been performed. Convective heating boundary condition are used to show the effects of impermeability of the stretching surface as well as the Soret diffusivity. Indeed, this result when compared with the previously published studies it was concurrently in line with them. Publications such as Mushtaq et al. (2014), Madaki et al. (2019) and Hussaini et al. (2020) for the sake of comparison some physical parameters of this study are considered to be zero. These are some of the conclusions we derived from the research;

1) The reduced Nusselt number (*Nur)* decreases significantly with Heat generation/absorption parameter and Biot number, the Sherwood number notably remained constant for each value.

2) The temperature and concentration remained constant for whatever values of Magnetic Parameter (M) and Eckert number (Ec).
3) The temperature decreases significantly while concentration profile remained constant with an increase in the values for Prandtl number (Pr) and magnetic parameter (M).
4) Moreover, the temperature gradient decreases with an increase in the values of Prandtl number and magnetic parameter.
5) The fluid's Velocity is physically reducing with the increase of Magnetic parameter irrespective of the value of impermeability parameter.
6) The fluid's Nusselt number physically decreases with the increment of Magnetic parameter.
7) The fluid's Sherwood number is physically decreasing with an increase of magnetic parameter not minding the values of impermeability parameter (increase/decrease).
8) The fluid's Temperature is decreasing with increase in Soret diffusivity parameter when the wall Temperature is decreased. Whereas, the fluid's temperature increases with increment of Soret diffusivity parameter when the wall temperature is increased.
9) The fluid's concentration increases with the increment in the value of Soret diffusivity irrespective of either increase or decrease in the value of the wall temperature.
10) Furthermore, the Nusselt number decreases significantly with the increment in the values of Soret diffusivity.
11) An increase in the value of heat generation ($\lambda > 0$), as well as the Soret diffusivity parameter produces an increase in the Sherwood number while the Sherwood number decreases with an increase in the value of heat absorption ($\lambda < 0$) and Soret diffusivity parameter respectively.
12) An increase in the values of impermeability parameter produces a decrease in the temperature profile irrespective of heat generation or hear absorption.

References

Abbasi, F. M., Shehzad, S. A., Hayat, T., & Ahmad. B. (2016). Doubly stratified mixed convection flow of Maxwell nanofluid with heat generation/absorption, *J. Magn. Magn. Mater*, 404, 159–65.

Ahmad, K., & Nazar, R. (2011). Magnetohydrodynamic threedimensional

flow and heat transfer over a stretching surface in a viscoelastic fluid, *J. science and technology*. 3, 1- 12.

Buongiorno, J. (2006). Convective transport in nanofluids, *J. Heat Transfer*, 128, 240–50.

Choi, S.U.S. (1995). Enhancing thermal conductivity of fluids with nanoparticles, *ASME, USA* 99–105, FED 231/MD.

Hayat, T., Farooq, M., & Alsaedi, A. (2015). Thermal radiation effect in MHD flow of Powell– Eyring nanofluid induced by a stretching cylinder, *Open Phys.* 13, 188–197.

Hussaini, A. A., Madaki, A.G., & Kwami A.M. (2021). Modified Mathematical Model on the Study of Convective MHD Nanofluid flow with Heat Generation/Absorption, *Int. J. of Engineering research and technology*, 10 (09), 155- 163.

Jawad, M., Shah, Z., Islam, S., Khan, W., & Khan, A.Z. (2019). Nanofluid thin film flow of Sisko fluid and variable heat transfer over an unsteady stretching surface with external magnetic field, *J. Algorithm Comput. Technol.* 13, 1 to 16.

Khan, W. A., & Pop I. (2010). Boundary-layer flow of a nanofluid past a stretching sheet. *Int. J. Heat Mass Transfer.* 53, 2477–2483.

Khan, W.A., Ali, M., Waqas, M., Shahzad, M., Sultan, F., & Irfan, M. (2019). Importance of convective heat transfer in flow of non-Newtonian nanofluid featuring Brownian and thermophoretic diffusions, *Int. J. Numer. Methods Heat Fluid Flow,* 29 (12) 4624 to 4641.

Madaki, A. G., Yakubu, D. G., Adamu, M. Y., & Roslan, R. (2019). The study of MHD Nanofluid flow with chemical reaction along with thermophoresis and Brownian motion on boundary layer flow over a linearly stretching sheet, *J. of pure and applied sci 19, 83 – 91*

Madaki, A.G., Roslan, R., Rusiman, M.S., Raju C.S.K. (2018). Analytical and numerical solutions of squeezing unsteady Cu and TiO2-nanofluid flow in the presence of thermal radiation and heat

generation/absorption, *Alexandria Engineering J., 57, 1033-1040*

Mabood, F., Ibrahim, S.M., & Khan, W.A. (2019). Effect of melting and heat generation/absorption on Sisko nanofluid over a stretching surface with nonlinear radiation, *Phys. Scripta* 94 (6), 1-11, https: //doi.org/10.1088/1402-4896/ab1164.

Macha, M., Reddy, C.S., & Kishan, N. (2017). Magnetohydrodynamic flow and heat transfer to Sisko nanofluid over a wedge, *Int. J. Fluid Mech. Res.* 44(1) 1 to 13, https://doi.org/10.1615/InterJFluidMechRes. 2017015861.

Makinde, O. D., & Aziz, A. (2011). Boundary layer flow of a nanofluid past a stretching sheet with a convective boundary condition, *Int. J. Therm. Sci*. 50, 1326–1332.

Makinde, O. D., Khan, W. A, & Khan ZH. (2013). Buoyancy effects on MHD stagnation point flow and heat transfer of a nanofluid past a convectively heated stretching/ shrinking sheet, *Int. J. Heat Mass Transfer*. 62, 526–533.

Nadeem, S., Haq, R.U., & Lee, C. (2012). MHD flow of a Casson fluid over an exponentially shrinking sheet, *Scientia Iranica*. 19, 1550–1553.

Pal, D., Mandal, G., & Vajravalu, K. (2019). Magnetohydrodynamic nonlinear thermal radiative heat transfer of nanofluids over a flat plate in a porous medium in existence of variable thermal conductivity and chemical reaction, *Int. J. Ambient Energy*, 1-30, https: //doi.org/10.1080/01430750.2019.1592776.

Shaw, S., Gorla, R.S.R., Murthy, P.V.S.N., & Ng, C-O. (2009). Pulsatile Casson fluid flow through a stenosed bifurcated artery, *Int. J. Fluid Mechanics Research.* 36(1), 43-63. http://dx.doi.org/10.1615/InterJFluidMechRes.v36.i1.30.

Sheikholeslami, M. Abelman, S., & Ganji, D. D. (2014). Numerical simulation of MHD nanofluid flow and heat transfer considering viscous dissipation, *Int. J. Heat Mass Transfer.* 79, 212–222.

Turkyilmazoglu, M. (2012). Exact analytical solutions for heat and mass

transfer of MHD slip flow in nanofluids, *Chem. Eng. Sci.* 84, 182–187.

Zeeshan, A., Baig, M., Ellahi, R., & Hayat, T. (2014). Flow of viscous nanofluid between the concentric cylinders, *J. Comput. Theor. Nanosci.*, 11, 646–54.